5066 *Biochemistry* **2009,** *48,* 5066–5073
DOI: 10.1021/bi900085v

BIOCHEMISTRY
including biophysical chemistry & molecular biology
Article

Deletion of ^{54}FLRAPSWF^{61} Residues Decreases the Oligomeric Size and Enhances the Chaperone Function of αB-Crystallin[†]

Puttur Santhoshkumar,[‡] Raju Murugesan,[‡] and K. Krishna Sharma*[,‡,§]

[‡]*Departments of Ophthalmology and* [§]*Biochemistry, University of Missouri, Columbia, Missouri 65212*

Received January 20, 2009; Revised Manuscript Received April 23, 2009

ABSTRACT: αB-Crystallin is a member of the small heat shock protein family and is known to have chaperone activity. Using a peptide scan approach, we previously determined that regions 42−57, 60−71, and 88−123 in αB-crystallin interact with αA-crystallin during heterooligomer formation. To further characterize the significance of the N-terminal domain of αB-crystallin, we prepared a deletion mutant that lacks residues ^{54}FLRAPSWF^{61} (αBΔ54−61) and found that the absence of residues 54−61 in αB-crystallin significantly decreased the homooligomeric mass of αB-crystallin. The average oligomeric mass of wild-type αB-crystallin and of αBΔ54−61, calculated using multiangle light scattering, was 624 and 382 kDa, respectively. The mutant subunits aggregate to form smaller, less-compact oligomers with a 4-fold increase in subunit exchange rate. Deletion of the 54−61 region resulted in a 50% decrease in intrinsic tryptophan fluorescence. The αBΔ54−61 mutant showed a 2-fold increase in 1,1′-bi(4-anilino)naphthalene-5,5′-disulfonic acid (bis-ANS) binding as compared to the wild-type protein, suggesting increased hydrophobicity of the mutant protein. Accompanying the evidence of increased hydrophobicity in the deletion mutant was a 10-fold increase in antiaggregation activity. Homooligomers of 6HαA (750 kDa) readily exchanged subunits with αBΔ54−61 homooligomers at 37 °C, forming heterooligomers with an intermediate mass of 625 kDa. Our data suggest that residues ^{54}FLRAPSWF^{61} contribute to the higher order assembly of αB-crystallin oligomers. Residues ^{54}FLRAPSWF^{61} in αB-crystallin are not essential for target protein binding during chaperone action, but this region apparently has a role in the chaperone activity of native αB-crystallin.

The major protein of the vertebrate eye, α-crystallin, belongs to the family of widely distributed proteins called small heat shock proteins (sHSPs).[1] The oligomer of α-crystallin is composed of two types of 20 kDa subunits, αA- and αB-crystallin, in the ratio ~3:1. The oligomer is polydisperse in nature and has a mass of 300−1200 kDa (*1*). Although, αA- and αB-crystallins were originally thought to be eye lens proteins exclusively, they were subsequently discovered to exist in many other tissues (*2*). In addition, their concentration was found to be increased in some disease conditions (*3*). The crystallin subunits have highly conserved sequences that show a high degree of homology to other sHSPs at the α-crystallin domain (*4*, *5*). Studies have so far led to limited structural information on sHSPs (*6*). The crystal structure identified for Hsp16.5 (*7*) has enabled homology modeling studies on αB-crystallin. However, inferences drawn from such studies cannot be relied upon completely because, unlike Hsp16.5, α-crystallins have a variably asymmetrical and highly polydispersed structure.

Oligomerization of sHsp subunits is essential in order for α-crystallins to function as molecular chaperones (*8*, *9*). Biophysical studies (*10*, *11*) and subunit interaction studies using peptide array (*12*) and pin array (*13*) suggest that extensive contact occurs between the subunits. Earlier we reported that 42−57 and 60−71 regions in αB-crystallin function as subunit interaction sites (*12*, *14*). Ghosh et al., in their pin array study, concluded that sequences 37−54, 75−82, 131−138, 141−148, and 155−166 in αB-crystallin are involved in subunit interaction (*13*). These investigators also used the pin array technique to determine the target protein interaction sites in αB-crystallin and reported that several sites in αB-crystallin function as chaperone sites (*15*). Of these sites, regions 43−58, 75−82, 131−138, 141−148, and 157−164 were reported to contain residues that overlap with the subunit interaction sites. A two-hybrid system study investigated the involvement of N- and C-terminal domains in subunit interaction and showed that in αB-crystallin only the C-terminal region is interacting during oligomerization (*16*, *17*).

Both the refractive role of α-crystallin and its chaperone-like property are thought to be essential for maintaining lens transparency. A large body of evidence suggests that mutations in α-crystallin subunits underlie loss of chaperone activity and,

[†]This work was supported by NIH Grant EY 11981 and an unrestricted grant from Research to Prevent Blindness to the Department of Ophthalmology of the University of Missouri.

*Address correspondence to this author at the Department of Ophthalmology, University of Missouri. Tel: 573-882-8478. Fax: 573-884-4100. E-mail: Sharmak@health.missouri.edu.

[1]Abbreviations: ADH, alcohol dehydrogenase; CS, citrate synthase; bis-ANS, 1,1′-bi(4-anilino)naphthalene-5,5′-disulfonic acid; CD, circular dichroism; FRET, fluorescence resonance energy transfer; sHSPs, small heat shock proteins; MALS, multiangle light scattering; PCR, polymerase chain reaction; PDI, polydispersity index; UV, ultraviolet.

 Published on Web 04/23/2009

in turn, may result in loss of lens transparency (*18*−*23*). Using novel cross-linkers and hydrophobic probes, we have shown that specific residues in the α-crystallin domain of αB-crystallin function as substrate interaction sites (*24*, *25*). This observation was later confirmed by the synthesis and characterization of a peptide that represents the chaperone site (*26*, *27*).

Site-directed mutagenesis studies by us and others show that both the N-terminal region and C-terminal region are involved in α-crystallin oligomerization (*10*, *12*, *14*, *28*−*32*). We showed that inversion of the 54−60 sequence in αB-crystallin affects the subunit interaction but does not alter its chaperone activity (*33*). An αBΔ41−58 mutant, characterized by Ghosh et al., (*34*) showed increased molecular size, polydispersity, and varying chaperone activity. The αBΔ41−58 mutant was less effective than wild-type αB-crystallin in protecting maximally unfolded citrate synthase (CS), whereas it was as effective as wild-type αB-crystallin in protecting partially unfolded *β*L-crystallin.

Residues 54−60 contribute to the sequences identified as the subunit interaction sites (*33*) as well as the chaperone site (*15*) in previous studies. Additionally, the αBR56 substitution or deletion study has shown that this residue plays a role in αB-crystallin structure−function (*35*). In this study, we characterized the αB-crystallin mutant in which residues 54−61 were deleted to determine the consequences of loss of this region. We show that αB-crystallin without residues 54−61 (a) forms a smaller homo-oligomer, (b) has fewer subunits per oligomer, (c) still interacts with αA-crystallin to form a smaller than normal size hetero-oligomer, and (d) is an efficient chaperone.

EXPERIMENTAL PROCEDURES

Construction, Expression, and Purification of Wild-Type αB-, αBΔ54−61, and 6HαA-Crystallins. Human αA- and αB-crystallin cDNA were cloned into pET23d vector (Novagen-EMD Biosciences, La Jolla, CA) at the *Nco*I/*Hin*dIII site. The αBΔ54−61 mutant (Figure 1) was constructed from the human αB-crystallin cDNA using the QuikChange site-directed mutagenesis kit (Stratagene, La Jolla, CA). The mutation was confirmed by DNA sequencing. The proteins were expressed in *Escherichia coli* BL21(DE3)pLysS cells (Invitrogen Corp., Carlsbad, CA), as described previously (*24*). To prepare His-tagged αA (6HαA), we used pQE-30 vector (Qiagen, Valencia, CA). *Bam*HI and *Pst*I restriction sites were introduced in αA-crystallin cDNA using polymerase chain reaction (PCR) to clone into pQE-30 vector. A second PCR was performed to correct the reading frame, and the sequence was verified by DNA sequencing. The protein was expressed in *E. coli* M15[pREP4] strain (Qiagen, Valencia, CA). The 6HαA prepared from this clone had an RGS-HHHHHH tag at the N-terminal end of the protein. His-tagged protein was isolated in native condition and purified using the QIAexpress system (Qiagen, Valencia, CA). The eluate was treated with 100 mM EDTA and purified further on a Superdex G200 column.

Structural Characterization of Wild-Type αB-Crystallin and αBΔ54−61. The purified proteins were spectroscopically analyzed to see if deletion of residues 54−61 leads to significant changes in αB-crystallin structure. Phosphate buffer (0.05 M) containing 0.15 M NaCl and 0.02% sodium azide (pH 7.4) was used in all measurements unless otherwise specified. The molecular mass of recombinant 6HαA- and αB-crystallins and of heterooligomers formed by a mixture of αA-crystallin and αBΔ54−61 was determined using a Biosep-sec4000 column.

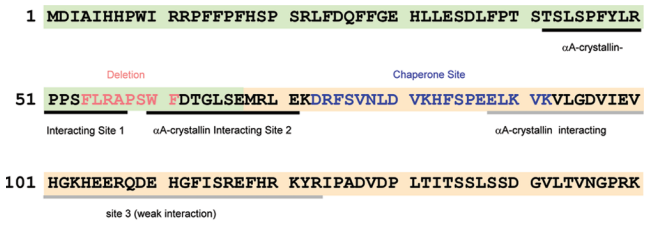

FIGURE 1: Amino acid sequence of human αB-crystallin showing the deleted ^{54}FLRAPSWF^{61}region: N-terminal domain (green shaded), α-crystallin domain (orange shaded), and C-terminal tail (yellow shaded). The putative αA-crystallin interacting sites and the chaperone site identified by us earlier are also shown. The residues deleted in this study are shown in red.

The intrinsic tryptophan fluorescence spectra of the wild-type and mutant αB-crystallins were recorded using a Jasco FP-750 spectrofluorometer, as described previously (*24*). The excitation wavelength was set to 295 nm, and the emission was recorded between 310 and 380 nm. Protein samples of 200 *μ*g/mL in phosphate buffer were used.

The solvent-exposed hydrophobic sites in the wild-type αB and αBΔ54−61 were probed using a hydrophobic dye, 1,1′-bi-(4-anilino)naphthalene-5,5′-disulfonic acid (bis-ANS) (Molecular Probes, Inc., Eugene, OR). A stock solution of the dye (14.8 mM) was prepared in 95% ethanol. To 200 *μ*g of wild-type and mutant αB-crystallins in 1 mL of phosphate buffer was added 10 *μ*L of bis-ANS stock solution. The mixture was incubated at 37 °C for 30 min. The interactions of bis-ANS with wild-type and mutant αB-crystallins were examined by recording the emission spectra between 450 and 600 nm. The samples were excited at 385 nm.

Changes in secondary and tertiary protein structures were investigated by measuring at room temperature far-ultraviolet (UV) and near-UV circular dichroism (CD) using the Jasco 815-CD spectrometer. Protein concentrations of 3.0 and 0.2 mg/mL in phosphate buffer were used for near- and far-UV CD measurements, respectively. The path length was 5 mm. The proteins were scanned eight times, the spectra were averaged, and the molar ellipticity of the mutant was compared with that of wild-type αB-crystallin.

Light Scattering. Protein samples were injected into a TSK G5000PW$_{XL}$ (Tosoh Bioscience, Montgomeryville, PA) size-exclusion column fitted to an HPLC with RID detector (Shimadzu Scientific Instruments, Inc., Columbia, MD) and equilibrated with phosphate buffer. The flow rate was set at 0.75 mL/min. The HPLC was coupled to multiangle light scattering (MALS) (DAWN) and quasi-elastic light scattering detectors (Wyatt Technology Corp., Santa Barbara, CA).

Transmission Electron Microscopy. A 5 *μ*L aliquot of the sample (2 mg/mL) was placed on a carbon-coated copper grid and allowed to absorb. After 1 min the excess sample was removed using a filter paper, and the grid was air-dried before negatively staining with 2% uranyl acetate for 2 min. The excess stain was removed from the grid, air-dried, and observed in a JEOL 1400 transmission electron microscope.

Subunit Interaction Studies. To demonstrate the presence of subunit exchange between αBΔ54−61 and 6HαA-crystallin, we labeled αBΔ54−61 with Alexa Fluor-350 dye (Molecular Probes Inc., Eugene, OR). Unlabeled 6HαA (250 *μ*g) and labeled αBΔ54−61 (75 *μ*g) were mixed (200 *μ*L) and incubated at 37 °C

for 3 h and then injected into an HPLC fitted with a TSK4000 gel filtration column and equilibrated with phosphate buffer. The flow rate was set at 0.5 mL/min. Another set of samples containing the same amounts of 6HαA and αBΔ54−61 was injected immediately (0 h) after mixing to obtain the elution profile of the individual proteins. The elution of the proteins was monitored using UV and fluorescent detectors, and the fractions were collected at 1 min intervals. The samples were then concentrated and analyzed on a SDS−PAGE.

FRET Assay. The subunit exchange rate of the proteins was determined by performing FRET assay. Labeling of the proteins was performed as described earlier (*12*), except that the unlabeled dye was removed by extensive dialysis. Proteins conjugated with Alexa Fluor-350 served as energy donors, while proteins conjugated with Alexa Fluor-488 acted as energy acceptors. Equal amounts (25 μg) of the labeled proteins were mixed in a total of 250 μL of phosphate buffer. The sample was incubated at 37 °C. The subunit exchange was monitored by exciting the sample at 346 nm and measuring the emission spectra from 400 to 600 nm at various intervals for up to 1.5 h. The subunit exchange rate was calculated from the FRET assay, as described previously (*10*).

Chaperone Assay. Chaperone-like activity of wild-type αB and the deletion mutant was compared using alcohol dehydrogenase (ADH) (Worthington) and CS (Sigma) substrates, as described previously (*24*, *36*). Aggregation of substrate proteins was monitored by measuring light scattering at 360 nm in the presence of various amounts of wild-type and mutant proteins as a function of time, using a Shimadzu spectrophotometer equipped with a temperature-regulated multicell holder.

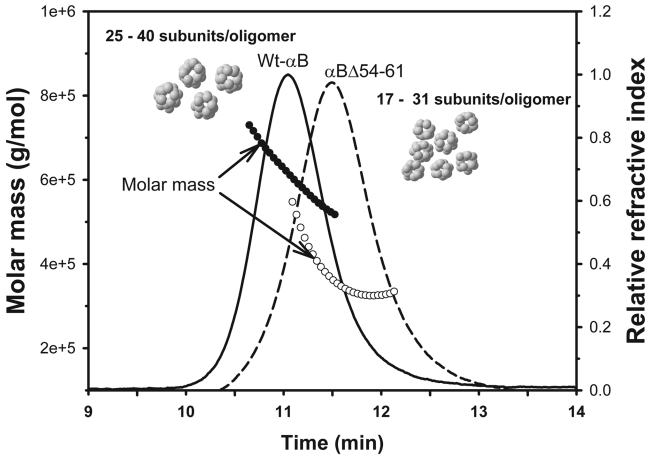

Protein	Mass distribution across peak (g/mol)	Mass (Mw) at the peak apex (g/mol)	Hydrodynamic radius, Rh (nm)	PDI	Average no. of subunits/ oligomer
Wt-αB	$7.91e^5$ - $5.18e^5$	$6.24 \pm 0.03e^5$	7.1	1.012	31
αBΔ54-61	$5.98e^5$ - $3.37e^5$	$3.82 \pm 0.03e^5$	6.8	1.025	20

FIGURE 2: Dynamic light scattering analysis of wild-type αB-crystallin (solid line, filled circle) and the αBΔ54−61 mutant (broken line, open circle). Proteins (0.15 mg in 0.05 mL) were incubated at 37 °C for 1 h prior to analysis. The molar mass distribution across the refractive index peaks, the polydispersity index (PDI), and the hydrodynamic radius of the proteins were analyzed from the MALS data using ASTRA (v5.3.2.10) software. The number of subunits per oligomer was calculated by dividing the oligomeric mass with the mass of the individual subunit.

RESULTS AND DISCUSSION

Numerous studies have shown that both the N- and C-terminal domain of α-crystallin subunits participate in hetero- and homooligomer formation (*10*, *12*, *15*, *28*, *31*, *34*, *37*, *38*). Previously, we demonstrated that residues 42−57 and 60−71 at the N-terminal domain of αB-crystallin are involved in subunit interactions (*12*) and designated these regions as recognition sites I and II (RS-1 and RS-2), respectively (Figure 1). We had also observed that inversion of the sequence 54−60 caused a 12% decrease in oligomer size of αB-crystallin but had no effect on chaperone-like activity of the protein (*33*). These data suggest that the RS-1 and RS-2 sequences along with the residues separating these two recognition sites play a role in αB-crystallin oligomerization.

Deletion of Residues 54−61 Leads to Smaller Homo-oligomers. In the present study we expressed the deletion mutant of αB-crystallin, αBΔ54−61, in *E. coli* BL21(DE3)pLysS cells and purified the protein by a combination of gel and ion-exchange chromatography. Deletion of residues 54−61 did not affect the solubility of the protein. The purity of the recombinant protein was confirmed by SDS−PAGE and mass spectrometry. During mass spectrometric analysis the mutant protein showed an expected mass of 19154 Da, confirming the deletion of residues 54−61. The deletion of the ^{54}FLRAPSWF^{61} sequence in αB-crystallin decreased the average oligomer size to 380 kDa (~20 subunits/oligomer mass), as compared to 620 kDa (~31 subunits/oligomer) for the wild-type protein (Figure 2). Surprisingly, approximately a 5% decrease (<1000 Da) in subunit mass resulted in a significantly larger decrease (about 39%) in oligomeric mass. This is likely due to the reduction in the number of mutant subunits that assemble to form an oligomer. It is not clear at this time what factor(s) limit(s) the number of subunits in the oligomer formed by the mutant αB-crystallin, but the results of this study suggest that the residue(s) within 54−61 region has (have) a role in the determination of oligomer size and the number of subunits forming this oligomer. The decreased oligomeric size of the αBΔ54−61 protein is also evident from the transmission electron micrographs (Figure 3). The wild-type αB-crystallin subunits are tightly packed to form compact oligomers (Figure 3A). In contrast, the αBΔ54−61 subunits are loosely packed, resulting in a less compact oligomer assembly (Figure 3B). The mutant subunits readily interact with the wild-type αB subunits to form intermediate-sized oligomers (Figure 3C).

Other investigators have observed a similar decrease (38%) in the oligomeric mass of αB-crystallin with deletion of residues 21−29 (*28*). Since the 21−29 region in αB-crystallin is not considered a subunit interaction region (*12*, *13*), the reason for the decrease in the oligomer size is unclear. In the same study (*28*) the authors reported a decrease in the hydrodynamic radius and polydispersity of the αBΔ21−29 mutant. We observed a decrease in the hydrodynamic radius and an increase in the polydispersity index (PDI) of the αBΔ54−61 mutant when compared to the wild-type protein (Figure 2). The reasons for the increased polydispersity in αBΔ54−61 are not known at this time. It could be due to increased subunit exchange rate (discussed below) that leaves the oligomers at various stages of assembly. Further studies are needed to confirm this hypothesis. Unlike αBΔ54−61 or αBΔ21−29 proteins, another deletion mutant (αBΔ41−58), characterized by Ghosh et al. (*34*), displayed increased oligomeric mass and polydispersity. This difference could be due to the length of deletion and the charge: deletion of 18 residues (including two Arg) as compared to deletion of 8 residues (including one Arg) in the current study. Studies with another

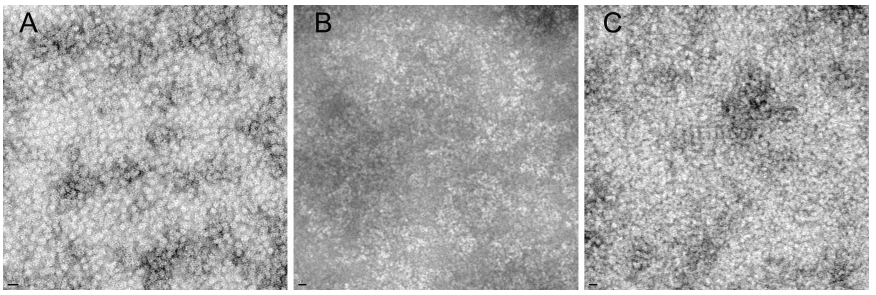

FIGURE 3: Transmission electron micrographs of wild-type and mutant αB-crystallins. A drop of 1 mg/mL protein was negatively stained with 2% uranyl acetate and observed under the JEOL 1200EX electron microscope. (A) Wild-type αB-crystallin; (B) αBΔ54−61; (C) αB wild type + αBΔ54−61 (1:1). Bar on the left corner in panels A, B, and C = 20 nm.

sHsp, Hsp16.5, have shown that the N-terminal region plays a critical role in determining oligomer size and polydispersity (*39*). Insertion of a 14 amino acid sequence into the N-terminal region of Hsp16.5 resulted in the assembly of a larger polydispersed oligomer. Previous study has shown that R56 substitution and deletion have paradoxical effects on the structure and function of αB-crystallin (*35*). While deletion of R56 resulted in increased chaperone activity, the substitution with Ala (αBR56A) led to nearly complete loss of chaperone activity. The αB 54−61 sequence having R56 is analogous to the 14-mer from sHsp27 used to convert the Hsp 16.5 to a larger oligomer. We observed that deletion of the 54−61 sequence from αB-crystallin was sufficient to generate a relatively smaller oligomer with increased chaperone activity. The oligomers formed from αBΔ54−61, however, showed increased polydispersity.

Structural Characterization of the αBΔ54−61 Mutant. The mutant and wild-type αB-crystallins showed significantly different tryptophan emission spectra (Figure 4A). While the maximal emission was found at 342 nm for both wild-type and mutant αB-crystallins, tryptophan fluorescence intensity was reduced by 50% in the αBΔ54−61 mutant. The reduction in tryptophan fluorescence was comparable to the previously observed decrease in the intrinsic fluorescence when residues 54−60 were inverted in αB-crystallin (*33*) or when W60 was mutated to arginine (*14*). In the present study the reduction in intrinsic fluorescence of the mutant can be attributed to the loss of one of the two tryptophan residues in αB-crystallin at the time of deletion whereas the quenching of fluorescence of tryptophan 54 in αB-54−60^{invert} likely contributed to the decrease in intrinsic fluorescence in the mutant protein (*33*). Subtle changes in protein structures that are not observed during CD analysis in some instances could lead to a change in Trp fluorescence (*40*). In this study the αBΔ54−61 with one Trp at the N-terminal region showed about one-half of the fluorescence of wild-type αB having two Trp residues. Therefore, it is unlikely that the environment of the N-terminal tryptophan was affected by the deletion.

To determine the impact of the deletion on the surface hydrophobicity of the protein, we investigated the ability of the mutant to bind the hydrophobic probe bis-ANS, whose fluorescence intensity increases and the emission maximum decreases upon binding to hydrophobic patches on the proteins (*41*). The fluorescence emission profile indicated that the mutant αB-crystallin has greater bis-ANS binding capacity than the wild-type protein (Figure 4B) although the deleted sequence was hydrophobic in nature. The subunit rearrangement that results in a smaller oligomer size may be responsible for the overall increase in hydrophobicity measured by bis-ANS. Perturbation of α-crystallin or of oligomers of αA- and αB-crystallin is known to lead to increased hydrophobicity (*42*). Earlier we observed

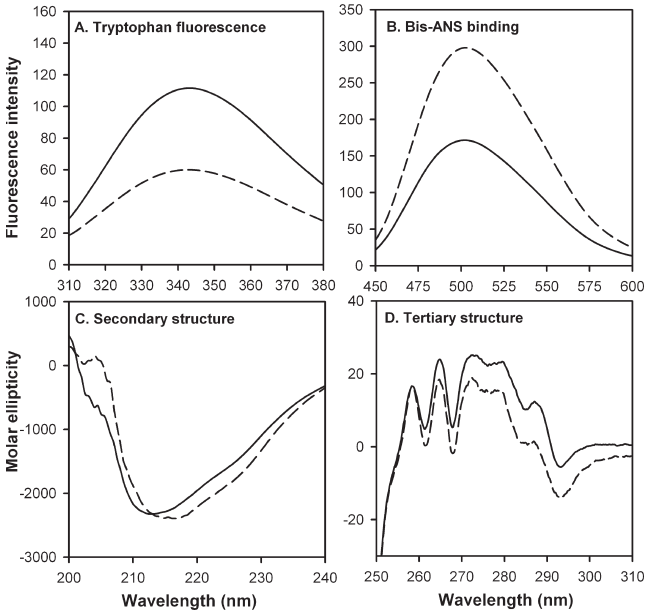

FIGURE 4: Spectroscopic characterization of wild-type αB-crystallin (solid line) and mutant αBΔ54−61 (broken line). (A) Tryptophan fluorescence intensity. Protein samples of 0.2 mg/mL in phosphate buffer were used. The excitation wavelength was set to 295 nm. (B) Bis-ANS binding. Bis-ANS stock, 10 μL (14.8 mM) solution, was added to 0.2 mg/mL protein in phosphate buffer and incubated at 37 °C for 30 min. The samples were excited at 385 nm. (C) Far-UV CD spectra were recorded at a protein concentration of 0.2 mg/mL using a 5 mm path length cell. (D) Near-UV CD spectra were recorded at a protein concentration of 3 mg/mL using a 5 mm path length cell.

that, in the mutant αB54−60^{invert} protein, the overall hydrophobicity was decreased marginally (<10%) in spite of the reduction in oligomer size and the change in tryptophan environment (*33*). C-Terminal truncation of αA-crystallin (αA-172) results in about 30% increase in hydrophobicity without a significant change in near- and far-UV spectra of mutant proteins (*43*).

The consequence of deletion of 54−61 residues on the structure of αB-crystallin was examined by both near- and far-UV CD spectral analysis of the protein (Figure 4C,D). The mutant protein and the wild-type protein showed similar negative ellipticity between 210 and 220 nm, but the peak for the mutant was at 216 nm whereas the peak for wild-type protein was at 212 nm. However, insignificant differences between the two proteins were found on analysis of α-helix, β-sheet, β-turn, and the amount of unordered structure (data not shown). The near-UV CD spectra of the mutant αB-crystallin showed characteristics similar to those of the wild-type protein except that the amplitude of the CD spectra between 275 to 290 nm was

slightly lower in the mutant protein. The minimal change was not surprising in the far- and near-UV CD spectra of αBΔ54−61 because the αBΔ41−58 mutant characterized by Ghosh et al. (*44*) also showed minimal changes in the far- and near-UV CD spectra. However, it was shown earlier that the αBR56A mutant shows significant changes in far- and near-UV spectra (*35*).

Deletion of Residues 54−61 Increases the Subunit Exchange Rate of αB-Crystallin. We previously proposed that residues 42−57 and 60−71 in αB-crystallin participate in subunit interaction (*12*). In the present study we investigated the effect of deletion of the 54−61 region on subunit interaction, subunit exchange, and oligomerization with the use of Alexa-350-labeled αB-crystallin and Alexa-488-labeled αBΔ54−61 crystallin. FRET analysis showed that mutant αB and wild-type αB-crystallins readily exchange to form heterooligomers or homooligomers (Figure 5). FRET analysis of a 1:1 mixture of αB and αBΔ54−61 showed that the exchange rate between the two types of subunits was lower than the exchange rate between the αBΔ54−61 mutants. Further, the exchange rate between the wild-type subunits was about 4 times slower than that between mutant subunits (Figure 5). Additionally, the presence of a denaturing protein, ADH, during FRET assay resulted in a diminished exchange rate between wild-type and αBΔ54−61 proteins. This suggests that prior binding of a denaturing protein to αB-crystallin constrains the oligomer from the dynamic aggregation−dissociation−aggregation process. Other investigators have shown that prior binding of γ-crystallin to α-crystallin significantly reduces the oligomer exchange (*45*). The increased subunit exchange rate of the αBΔ54−61 mutant could be due to the decreased affinity between subunits as a consequence of loss of residues from the interacting region.

αBΔ54−61 Readily Interacts with αA-Crystallin To Form a Smaller than Normal Heterooligomer. We examined the interaction of αBΔ54−61 and αA-crystallin using 6HαA-crystallin and Alexa Fluor-350-labeled αBΔ54−61 by the gel filtration chromatographic method. As shown in Figure 6A, 6HαA eluted from the TSK4000 column with a peak at 30 min, whereas the Alexa-labeled αBΔ54−61 eluted later and peaked at 35 min. The elution positions of these proteins were confirmed by SDS−PAGE analysis of the TSK4000 eluants (Figure 6B, 0 h incubation samples). When 6HαA- and Alexa Fluor-labeled αBΔ54−61 were mixed and incubated for 3 h, a new peak with an elution time of 33−34 min emerged during gel chromatography. This peak showed both fluorescence and absorbance. SDS−PAGE analysis of the fractions eluting from the column showed that all of the fractions contained the same ratios of 6HαA- and αBΔ54−61. The data confirm that the deletion mutant readily forms a heterooligomer with αA-crystallin. Further, our study also suggests that αBΔ54−61 can control the size of a heterooligomer of αA- and αBΔ54−61. Peptide array data from our previous study revealed that residues 42−57 and 60−71 in αB-crystallin interact with αA-crystallin (*12*). The present data show that deletion of four residues from the 42−57 region and two residues from the 60−71 region does not affect the interaction of αB-crystallin with αA-crystallin. It is likely that the αBΔ54−61 mutant exhibits its full potential to interact with αA-crystallin because of the presence of additional interaction sites (*13*, *28*, *38*) or interaction via the remainder of the 42−57 and 60−67 regions offering a three-dimensional interface, whereas the peptides in array do not have the affinity required for the binding when they lose some of the amino acids that flank the critical residues involved in binding.

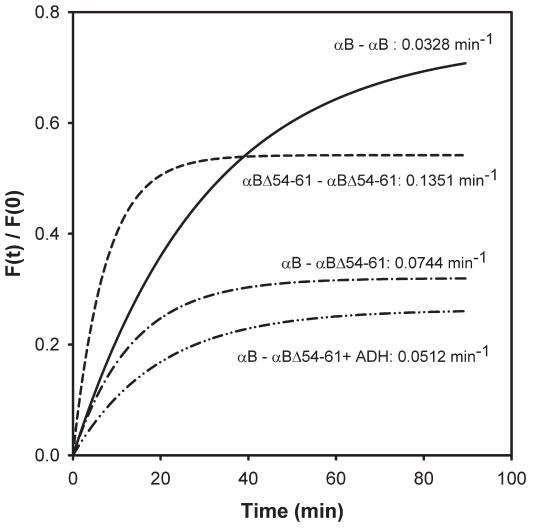

FIGURE 5: Subunit exchange studies of wild-type αB-crystallin and αB-Δ54−61 in the presence and absence of ADH. The labeled proteins were mixed in equal amounts (25 μg) in a total volume of 250 μL of phosphate buffer. To determine the effect of substrate on subunit exchange, ADH (150 μg) was incubated at 37 °C for 15 min prior to the addition of labeled chaperone proteins. The exchange rate is shown beside the graphs.

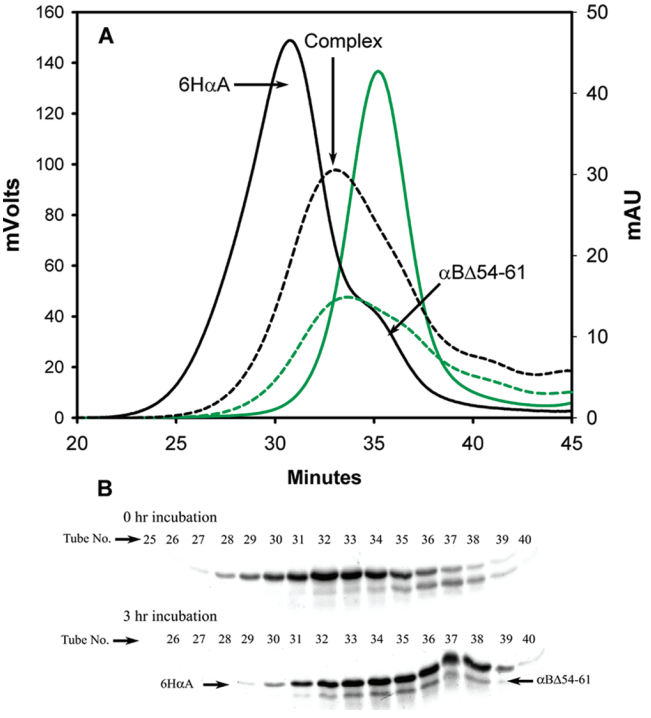

FIGURE 6: Demonstration of subunit interaction between 6HαA and αBΔ54−61. (A) Chromatographic profile of 6HαA (250 μg) and Alexa-350-labeled αBΔ54−61 mixture at 0 min time (solid line) and after 3 h (broken line) of incubation. The black lines represent the UV profile at 280 nm. The green lines represent the fluorescence profile. Prior to incubation the bulk of 6HαA and αBΔ54−61 elutes at 30 and 35 min, respectively. After 3 h of incubation, the proteins are largely seen coeluting at 33−34 min. (B) SDS−PAGE of fractions collected during chromatography. The tube numbers are offset by minutes due to delay in sample collection.

Deletion of Residues 54−61 Enhances the Chaperone-like Function of αB-Crystallin. Past studies with crystallin mutants showed that in most cases the increased hydrophobicity of a mutant is accompanied by increased chaperone-like activity (*28*, *46*). Other reports, however, showed no correlation between

binding of hydrophobic probes and chaperone-like activity of the protein (*47*, *48*). Because the deletion mutant in our present study showed increased bis-ANS binding, we determined whether the increased hydrophobicity has any impact on the chaperone-like activity by testing the ability of both wild-type and the mutant αB-crystallin to suppress EDTA-induced aggregation of ADH and heat-induced aggregation of CS using different ratios of αB and the denaturing proteins (Figure 7). During two different aggregation assays, the deletion mutant was found to have 10-fold greater chaperone-like activity than the wild-type protein. For example, only 4.5 μg of αBΔ54−61 was sufficient to suppress by 50% aggregation of 200 μg of ADH. In contrast, 46.3 μg of wild-type αB-crystallin was required for an equivalent degree of aggregation suppression. This observation suggests that deletion of residues 54−61 has a significant effect on the chaperone-like activity of the protein and correlates with the increased hydrophobicity of the mutant. Ghosh et al. (*15*) in their pin array study proposed that the 43−58 region in αB-crystallin is a common substrate protein interaction site or chaperone site. In a subsequent study (*44*), however, deletion of residues 41−58 was shown to have no effect on the chaperone-like activity of the protein when ADH or βL-crystallins were used as substrates. It should be noted that αBΔ41−58 produced heterogeneous oligomers with average molecular masses of 2437 and 420 kDa (*34*). It is not known whether the two kinds of oligomers showed similar chaperone activity. In a site-directed mutagenesis study of R56, deletion of the residues did not affect chaperone-like activity, whereas R56A mutation resulted in almost complete loss of chaperone-like activity (*46*).

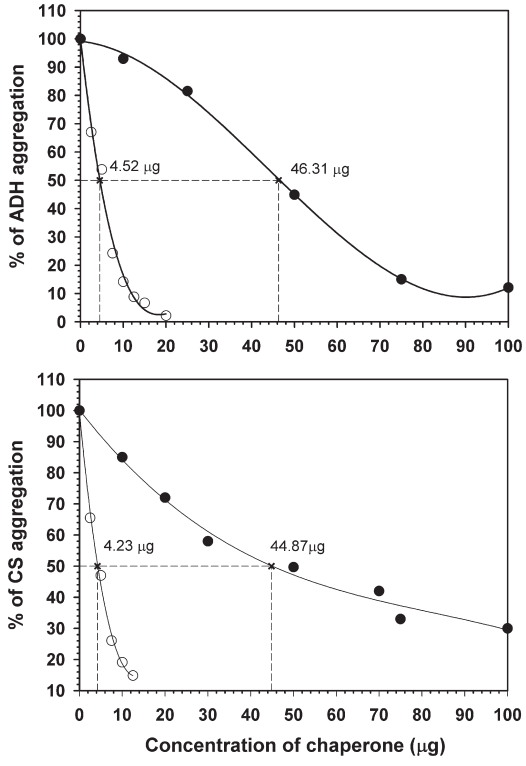

FIGURE 7: Comparison of antiaggregation activities of αBΔ54−61 and wild-type αB-crystallins using ADH and CS as substrate proteins. Aggregation of ADH (250 μg) was induced at 37 °C by phosphate buffer containing100 mM EDTA, and aggregation of CS (75 μg in 40 mM HEPES−NaOH buffer) was initiated by heating the sample at 43 °C. The percentage of substrate protein aggregated in the presence of various concentrations of wild type (solid circle) and αBΔ54−61 (open circle) was calculated at the 45 min time point and plotted. The aggregation of substrate protein in the absence of chaperone protein was considered 100% aggregation. The amount of chaperone protein required to prevent the aggregation of the substrate by 50% was calculated from the nonlinear regression analysis. This value is used to compare the chaperone efficiency of wild-type and mutant proteins.

We analyzed the reaction mixtures in chaperone assays by gel chromatography and DLS methods (Figure 8). Both wild-type and the deletion mutant of αB-crystallin formed complexes with denaturing ADH that were significantly larger than the ADH. The presence of ADH in the complex was confirmed by SDS−PAGE analysis (data not shown). The molar mass (M_w) of αBΔ54−61 + ADH at the complex peak apex was slightly larger than that of the αB + ADH complex. Since the M_w of αBΔ54−61 was significantly lower than that of wild-type αB-crystallin (Figure 2), we believe the increased chaperone activity of αBΔ54−61 (Figure 7) resulted in a marginally larger αBΔ54−61 + ADH complex due to increased ADH binding as compared to the αB + ADH complex. The αBΔ54−61 + ADH complex exhibited a higher hydrodynamic radius and polydispersity index (PDI) as compared to the αB + ADH complex.

At any given chaperone protein concentration, the αBΔ54−61 oligomers are 1.5 times in excess to αB oligomers. In addition to the increased number of αBΔ54−61 oligomers, the increased hydrophobicity of αBΔ54−61 and increased subunit exchange rate may also be contributing to the increased chaperone function of the deletion mutant. It is apparent from the data shown in Figures 7 and 8 that the αBΔ54−61 oligomers have increased capacity to bind denaturing proteins. It has been suggested that the dynamic state of crystallins dictates the chaperone activity of the protein (*49*), and a number of studies have shown that increased subunit exchange is associated with increased chaperone activity (*42*, *50*). It is possible therefore that the increased dissociation of oligomeric units coupled to increased subunit exchange rate observed in αBΔ54−61 may be contributing to the enhanced chaperone activity. The multiangle light scattering analysis of the complex suggests that the deletion mutant

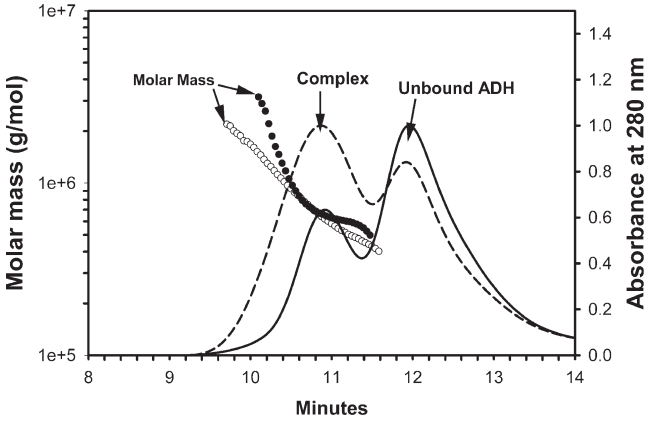

Proteins	Mass distribution in the complex peak (g/mol)	Molar mass (M_w) at the complex peak apex (g/mol)	Hydrodynamic radius (Rh) of the complex peak (nm)	PDI of the complex peak
αB + ADH	$3.45e^6 - 5.21e^5$	$7.28e^5$	9.2	1.089
αBΔ54-61 + ADH	$2.49e^6 - 3.99e^5$	$7.59e^5$	9.5	1.169

FIGURE 8: Molar mass distribution of wild-type αB-ADH (solid line, filled circle) and αB-Δ54−61-ADH (broken line, open circle). Crystallins and the ADH in equal concentration (50 μg) in phosphate buffer were incubated at 37 °C for 1 h, and the reaction mixtures were analyzed by MALS following TSK G4000PWxL chromatography. The table below the graph shows additional parameters determined during MALS measurements.

interacts with unfolding ADH more rapidly and forms aggregates with larger oligomeric mass and hydrodynamic radius than the wild-type ADH aggregate. The deletion of the 54−61 region might have activated cryptic chaperone sites or may have created additional chaperone site(s) in the oligomer. In an earlier study, methyl glyoxal modification of α-crystallin lead to increased chaperone activity (*51*), and this was attributed to increased hydrophobicity and subunit exchange rate. Further studies are required to identify the residues that contribute to the "new" sites. Whatever may be the reason for the increased chaperone activity, the results of this study demonstrate that the 54−61 region in αB-crystallin does not contribute to substrate binding. The increased chaperone activity of the deletion mutant may not be beneficial to αB-crystallin because the αBΔ54−61 + ADH complex has a higher PDI. We have observed that protein samples with higher PDI precipitate early (*52*). In another study involving αAR116C it has been suggested that increased chaperone activity may be responsible for the in vivo aggregation of crystallins and congenital cataractogenesis (*53*). αAR116C−client protein complexes are less stable than the αA−client protein complexes. Therefore, we conclude that residues ^{54}FLRAPSWF^{61} in αB-crystallin are required to form the stable chaperone−substrate complex, in addition to their contribution to higher order oligomeric assembly.

ACKNOWLEDGMENT

We thank Sharon Morey for help in the preparation of the manuscript.

REFERENCES

1. Horwitz, J. (2003) Alpha-crystallin. *Exp. Eye Res. 76*, 145–153.
2. Bhat, S. P., and Nagineni, C. N. (1989) alpha B subunit of lens-specific protein alpha-crystallin is present in other ocular and non-ocular tissues. *Biochem. Biophys. Res. Commun. 158*, 319–325.
3. Clark, J. I., and Muchowski, P. J. (2000) Small heat-shock proteins and their potential role in human disease. *Curr. Opin. Struct. Biol. 10*, 52–59.
4. Narberhaus, F. (2002) Alpha-crystallin-type heat shock proteins: socializing minichaperones in the context of a multichaperone network. *Microbiol. Mol. Biol. Rev. 66*, 64–93.
5. Sun, Y., and MacRae, T. H. (2005) Small heat shock proteins: molecular structure and chaperone function. *Cell. Mol. Life Sci. 62*, 2460–2476.
6. Bloemendal, H., de Jong, W., Jaenicke, R., Lubsen, N. H., Slingsby, C., and Tardieu, A. (2004) Ageing and vision: structure, stability and function of lens crystallins. *Prog. Biophys. Mol. Biol. 86*, 407–485.
7. Kim, K. K., Kim, R., and Kim, S. H. (1998) Crystal structure of a small heat-shock protein. *Nature 394*, 595–599.
8. Kokke, B. P., Leroux, M. R., Candido, E. P., Boelens, W. C., and de Jong, W. W. (1998) *Caenorhabditis elegans* small heat-shock proteins Hsp12.2 and Hsp12.3 form tetramers and have no chaperone-like activity. *FEBS Lett. 433*, 228–232.
9. Leroux, M. R., Melki, R., Gordon, B., Batelier, G., and Candido, E. P. (1997) Structure-function studies on small heat shock protein oligomeric assembly and interaction with unfolded polypeptides. *J. Biol. Chem. 272*, 24646–24656.
10. Bova, M. P., McHaourab, H. S., Han, Y., and Fung, B. K. (2000) Subunit exchange of small heat shock proteins. Analysis of oligomer formation of alphaA-crystallin and Hsp27 by fluorescence resonance energy transfer and site-directed truncations. *J. Biol. Chem. 275*, 1035–1042.
11. Berengian, A. R., Parfenova, M., and McHaourab, H. S. (1999) Site-directed spin labeling study of subunit interactions in the alpha-crystallin domain of small heat-shock proteins. Comparison of the oligomer symmetry in alphaA-crystallin, HSP 27, and HSP 16.3. *J. Biol. Chem. 274*, 6305–6314.
12. Sreelakshmi, Y., Santhoshkumar, P., Bhattacharyya, J., and Sharma, K. K. (2004) AlphaA-crystallin interacting regions in the small heat shock protein, alphaB-crystallin. *Biochemistry 43*, 15785–15795.
13. Ghosh, J. G., and Clark, J. I. (2005) Insights into the domains required for dimerization and assembly of human alphaB crystallin. *Protein Sci. 14*, 684–695.
14. Sreelakshmi, Y., and Sharma, K. K. (2005) Recognition sequence 2 (residues 60−71) plays a role in oligomerization and exchange dynamics of alphaB-crystallin. *Biochemistry 44*, 12245–12252.
15. Ghosh, J. G., Estrada, M. R., and Clark, J. I. (2005) Interactive domains for chaperone activity in the small heat shock protein, human alphaB crystallin. *Biochemistry 44*, 14854–14869.
16. Liu, C., and Welsh, M. J. (1999) Identification of a site of Hsp27 binding with Hsp27 and alpha B-crystallin as indicated by the yeast two-hybrid system. *Biochem. Biophys. Res. Commun. 255*, 256–261.
17. Fu, L., and Liang, J. J. (2002) Detection of protein-protein interactions among lens crystallins in a mammalian two-hybrid system assay. *J. Biol. Chem. 277*, 4255–4260.
18. Santhiya, S. T., Soker, T., Klopp, N., Illig, T., Prakash, M. V., Selvaraj, B., Gopinath, P. M., and Graw, J. (2006) Identification of a novel, putative cataract-causing allele in CRYAA (G98R) in an Indian family. *Mol. Vision 12*, 768–773.
19. Shroff, N. P., Cherian-Shaw, M., Bera, S., and Abraham, E. C. (2000) Mutation of R116C results in highly oligomerized alpha A-crystallin with modified structure and defective chaperone-like function. *Biochemistry 39*, 1420–1426.
20. Kumar, L. V., Ramakrishna, T., and Rao, C. M. (1999) Structural and functional consequences of the mutation of a conserved arginine residue in alphaA and alphaB crystallins. *J. Biol. Chem. 274*, 24137–24141.
21. Vicart, P., Caron, A., Guicheney, P., Li, Z., Prevost, M. C., Faure, A., Chateau, D., Chapon, F., Tome, F., Dupret, J. M., Paulin, D., and Fardeau, M. (1998) A missense mutation in the alphaB-crystallin chaperone gene causes a desmin-related myopathy. *Nat. Genet. 20*, 92–95.
22. Simon, S., Michiel, M., Skouri-Panet, F., Lechaire, J. P., Vicart, P., and Tardieu, A. (2007) Residue R120 is essential for the quaternary structure and functional integrity of human alphaB-crystallin. *Biochemistry 46*, 9605–9614.
23. Aquilina, J. A., Benesch, J. L., Ding, L. L., Yaron, O., Horwitz, J., and Robinson, C. V. (2004) Phosphorylation of alphaB-crystallin alters chaperone function through loss of dimeric substructure. *J. Biol. Chem. 279*, 28675–28680.
24. Santhoshkumar, P., and Sharma, K. K. (2006) Conserved F84 and P86 residues in alphaB-crystallin are essential to effectively prevent the aggregation of substrate proteins. *Protein Sci. 15*, 2488–2498.
25. Sharma, K. K., Kaur, H., and Kester, K. (1997) Functional elements in molecular chaperone alpha-crystallin: identification of binding sites in alpha B-crystallin. *Biochem. Biophys. Res. Commun. 239*, 217–222.
26. Sharma, K. K., Kumar, R. S., Kumar, G. S., and Quinn, P. T. (2000) Synthesis and characterization of a peptide identified as a functional element in alphaA-crystallin. *J. Biol. Chem. 275*, 3767–3771.
27. Bhattacharyya, J., Padmanabha Udupa, E. G., Wang, J., and Sharma, K. K. (2006) Mini-alphaB-crystallin: a functional element of alphaB-crystallin with chaperone-like activity. *Biochemistry 45*, 3069–3076.
28. Pasta, S. Y., Raman, B., Ramakrishna, T., and Rao Ch, M. (2003) Role of the conserved SRLFDQFFG region of alpha-crystallin, a small heat shock protein. Effect on oligomeric size, subunit exchange, and chaperone-like activity. *J. Biol. Chem. 278*, 51159–51166.
29. Kumar, L. V., and Rao, C. M. (2000) Domain swapping in human alpha A and alpha B crystallins affects oligomerization and enhances chaperone-like activity. *J. Biol. Chem. 275*, 22009–22013.
30. Eifert, C., Burgio, M. R., Bennett, P. M., Salerno, J. C., and Koretz, J. F. (2005) N-terminal control of small heat shock protein oligomerization: changes in aggregate size and chaperone-like function. *Biochim. Biophys. Acta 1748*, 146–156.
31. Thampi, P., and Abraham, E. C. (2003) Influence of the C-terminal residues on oligomerization of alpha A-crystallin. *Biochemistry 42*, 11857–11863.
32. Kundu, M., Sen, P. C., and Das, K. P. (2007) Structure, stability, and chaperone function of alphaA-crystallin: role of N-terminal region. *Biopolymers 86*, 177–192.
33. Sreelakshmi, Y., and Sharma, K. K. (2006) The interaction between alphaA- and alphaB-crystallin is sequence-specific. *Mol. Vision 12*, 581–587.
34. Ghosh, J. G., Shenoy, A. K.Jr., and Clark, J. I. (2006) N- and C-terminal motifs in human alphaB crystallin play an important role in the recognition, selection, and solubilization of substrates. *Biochemistry 45*, 13847–13854.
35. Biswas, A., Goshe, J., Miller, A., Santhoshkumar, P., Luckey, C., Bhat, M. B., and Nagaraj, R. H. (2007) Paradoxical effects of

substitution and deletion mutation of Arg56 on the structure and chaperone function of human alphaB-crystallin. *Biochemistry 46*, 1117–1127.
36. Santhoshkumar, P., and Sharma, K. K. (2001) Analysis of alpha-crystallin chaperone function using restriction enzymes and citrate synthase. *Mol. Vision 7*, 172–177.
37. Aquilina, J. A., Benesch, J. L., Ding, L. L., Yaron, O., Horwitz, J., and Robinson, C. V. (2005) Subunit exchange of polydisperse proteins: mass spectrometry reveals consequences of alphaA-crystallin truncation. *J. Biol. Chem. 280*, 14485–14491.
38. Pasta, S. Y., Raman, B., Ramakrishna, T., and Rao Ch, M. (2004) The IXI/V motif in the C-terminal extension of alpha-crystallins: alternative interactions and oligomeric assemblies. *Mol. Vision 10*, 655–662.
39. Shi, J., Koteiche, H. A., McHaourab, H. S., and Stewart, P. L. (2006) Cryoelectron microscopy and EPR analysis of engineered symmetric and polydisperse Hsp16.5 assemblies reveals determinants of polydispersity and substrate binding. *J. Biol. Chem. 281*, 40420–40428.
40. Fujii, N., Uchida, H., and Saito, T. (2004) The damaging effect of UV-C irradiation on lens alpha-crystallin. *Mol. Vision 10*, 814–820.
41. Sharma, K. K., Kaur, H., Kumar, G. S., and Kester, K. (1998) Interaction of 1,1′-bi(4-anilino)naphthalene-5,5′-disulfonic acid with alpha-crystallin. *J. Biol. Chem. 273*, 8965–8970.
42. Srinivas, V., Raman, B., Rao, K. S., Ramakrishna, T., and Rao Ch, M. (2003) Structural perturbation and enhancement of the chaperone-like activity of alpha-crystallin by arginine hydrochloride. *Protein Sci. 12*, 1262–1270.
43. Aziz, A., Santhoshkumar, P., Sharma, K. K., and Abraham, E. C. (2007) Cleavage of the C-terminal serine of human alphaA-crystallin produces alphaA1−172 with increased chaperone activity and oligomeric size. *Biochemistry 46*, 2510–2519.
44. Ghosh, J. G., Shenoy, A. K.Jr., and Clark, J. I. (2007) Interactions between important regulatory proteins and human alphaB crystallin. *Biochemistry 46*, 6308–6317.
45. Putilina, T., Skouri-Panet, F., Prat, K., Lubsen, N. H., and Tardieu, A. (2003) Subunit exchange demonstrates a differential chaperone activity of calf alpha-crystallin toward beta LOW- and individual gamma-crystallins. *J. Biol. Chem. 278*, 13747–13756.
46. Biswas, A., Miller, A., Oya-Ito, T., Santhoshkumar, P., Bhat, M., and Nagaraj, R. H. (2006) Effect of site-directed mutagenesis of methylglyoxal-modifiable arginine residues on the structure and chaperone function of human alphaA-crystallin. *Biochemistry 45*, 4569–4577.
47. Santhoshkumar, P., and Sharma, K. K. (2001) Phe71 is essential for chaperone-like function in alpha A-crystallin. *J. Biol. Chem. 276*, 47094–47099.
48. Kumar, M. S., Kapoor, M., Sinha, S., and Reddy, G. B. (2005) Insights into hydrophobicity and the chaperone-like function of alphaA- and alphaB-crystallins: an isothermal titration calorimetric study. *J. Biol. Chem. 280*, 21726–21730.
49. Datta, S. A., and Rao, C. M. (2000) Packing-induced conformational and functional changes in the subunits of alpha-crystallin. *J. Biol. Chem. 275*, 41004–41010.
50. Bova, M. P., Huang, Q., Ding, L., and Horwitz, J. (2002) Subunit exchange, conformational stability, and chaperone-like function of the small heat shock protein 16.5 from *Methanococcus jannaschii*. *J. Biol. Chem. 277*, 38468–38475.
51. Nagaraj, R. H., Oya-Ito, T., Padayatti, P. S., Kumar, R., Mehta, S., West, K., Levison, B., Sun, J., Crabb, J. W., and Padival, A. K. (2003) Enhancement of chaperone function of alpha-crystallin by methylglyoxal modification. *Biochemistry 42*, 10746–10755.
52. Santhoshkumar, P., Udupa, P., Murugesan, R., and Sharma, K. K. (2008) Significance of interactions of low molecular weight crystallin fragments in lens aging and cataract formation. *J. Biol. Chem. 283*, 8477–8485.
53. Koteiche, H. A., and McHaourab, H. S. (2006) Mechanism of a hereditary cataract phenotype. Mutations in alphaA-crystallin activate substrate binding. *J. Biol. Chem. 281*, 14273–14279.